Nonequilibrium Green's function picture of nonradiative recombination of the Shockley-Read-Hall type

Urs Aeberhard*

IEK-5 Photovoltaik, Forschungszentrum Jülich, D-52425 Jülich, Germany



(Received 30 October 2018; published 18 March 2019)

A quantum-kinetic picture of Shockley-Read-Hall-type (SRH) defect-mediated recombination is derived within the nonequilibrium Green's function formalism for an optoelectronic device with selectively contacted, current-carrying extended states and a localized deep defect state in the energy gap. The theory is first tested for recombination from bulk band states and then implemented for defective bipolar homo- and heterojunction thin-film devices with realistic spatial variation of the band edge profile. While the quantum-kinetic treatment reproduces the semiclassical characteristics for a bulk absorber in flat-band and quasiequilibrium conditions, for which the conventional SRH picture is valid, it reveals nonclassical features such as recombination enhancement by tunneling into field-induced subgap states in the presence of large fields, or the complex recombination current flow at heterointerfaces. Being fully compatible with the rigorous treatment of electron-photon and electron-phonon scattering in the nonequilibrium Green's function (NEGF) formalism, the approach enables a consistent inclusion of defect-mediated nonradiative recombination in comprehensive NEGF simulations of nanostructure-based quantum optoelectronic devices such as quantum well lasers, LEDs and solar cells.

DOI: 10.1103/PhysRevB.99.125302

I. INTRODUCTION

Many state-of-the-art architectures for optoelectronic devices ubiquitous in developed and sustainable societies, e.g., LEDs, lasers, and solar cells, rely on nanostructure components providing specific functionalities that are tunable via configurational parameters such as composition, size, and shape. However, the introduction of spatial inhomogeneities tends to promote the formation of structural or chemical defects, with detrimental impact on device performance when acting as recombination centers. Defect-mediated recombination hence needs to be considered in any device simulation approach aiming at the performance assessment of optoelectronic components under realistic conditions. Indeed, nonradiative recombination such as the one described by the Shockley-Read-Hall (SRH) formalism [1,2] is routinely included in conventional semiclassical simulations of bulk devices, e.g., by drift-diffusion models, for which the rates can even be obtained accurately from first principles, using density functional (perturbation) theory (DFT) [3-10] or, more recently, nonadiabatic molecular dynamics in combination with time-dependent DFT [11]. On the other hand, defect-mediated recombination processes are still missing in the more advanced and fundamental quantum device simulation approaches required to tackle the effects of confinement and tunneling present in nanostructure-based quantumoptoelectronic device architectures with complex potential landscapes, like the nonequilibrium Green's function formalism (NEGF) [12–26].

The present article extends the applicability of the well-established NEGF simulation framework for

quantum-optoelectronic devices [27,28] beyond the radiative limit by treating nonradiative, SRH-type recombination on equal footing with optical transitions and inelastic quantum transport. The basic idea—as presented first in Ref. [29]—is to couple isolated, localized defects via an inelastic scattering process to the system of current carrying extended states, and is thus similar to the NEGF theory of phonon-assisted optical transitions [30], where indirect excitations are enabled due to the modification of the charge carrier propagators in a self-consistency iteration procedure, or the description of two-step photogeneration via the photofilling of an intermediate state [28]. The resulting self-energy expressions are fully compatible with the self-consistent self-energy schemes for both the coherent and incoherent coupling of electrons to photons required for the description of stimulated and spontaneous radiative processes dominating the operation of solar cell devices, as described in Ref. [31], and the self-energies for electron-phonon scattering required for the consideration of intraband carrier relaxation processes relevant for inelastic quantum transport [32,33].

The paper is organized as follows. In Sec. II the description of defect-related quantities within the NEGF formalism is introduced. Based on this description, a general steady-state defect recombination rate is formulated in Sec. III. In Sec. IV the equivalence of this rate to the conventional SRH recombination rate is demonstrated for the special case of a bulk semiconductor with quasiequilibrium occupation. In Sec. V the theory is implemented and verified for the specific case of defect occupation mediated by multiphonon relaxation, first for bulk states and then for a homogeneous *p-i-n* device, before it is used to study the recombination current at an AlGaAs-GaAs heterointerface as encountered in high-efficiency GaAs solar cells [34].

^{*}u.aeberhard@fz-juelich.de

II. NEGF DESCRIPTION OF DEFECTS

Here an ensemble of strongly localized point defects will be considered. Electrons occupying such defect levels labeled by ν may be described by the field operator [35]

$$\hat{\Phi}(\mathbf{r},t) = \sum_{i,\nu} \phi_{i_d\nu}^d(\mathbf{r}) \hat{d}_{i_d\nu}(t), \tag{1}$$

where $\phi_{i_d v}^d$ is the defect wave function for defect i_d , which is localized around \mathbf{r}_{i_d} and will thus be approximated by

$$\phi_{i_d \nu}^d(\mathbf{r}) \approx c_{i_d \nu}^d \delta(\mathbf{r} - \mathbf{r}_{i_d}),$$
 (2)

where $c_{i_dv}^d = 1$ for nondegenerate states. Since the electrons in defect states are localized, the Hamiltonian of the isolated defect system consists merely of an on-site term,

$$\hat{H}_{d,(0)} = \sum_{i,\nu} \varepsilon_{i_d\nu}^d \hat{d}_{i_d\nu}^\dagger \hat{d}_{i_d\nu}.$$
 (3)

For simplicity we will consider in the following a single defect level only, at energy ε_d . For a general nonequilibrium situation, the corresponding Green's functions, which are the Fourier-transformed steady-state version of the real-time components of contour-ordered object $\mathcal{G}(t,t') = -\frac{i}{\hbar} \langle \hat{d}(t) \hat{d}^{\dagger}(t') \rangle_{\mathcal{C}}$, are the scalar quantities

$$G_{d,(0)}^{R,A}(E) = \{E \pm i\eta - \varepsilon_d\}^{-1},$$
 (4)

$$G_{d,(0)}^{<}(E) = if_d(E)A_{d,(0)}(E),$$
 (5)

$$G_{d,(0)}^{>}(E) = -i\{1 - f_d(E)\}A_{d,(0)}(E),$$
 (6)

where

$$A_{d,(0)}(E) = i \left\{ G_{d,(0)}^{R}(E) - G_{d,(0)}^{A}(E) \right\}$$
 (7)

$$\equiv i\{G_{d,(0)}^{>}(E) - G_{d,(0)}^{<}(E)\} \tag{8}$$

is the spectral function of the defect, and f_d describes the occupation of the defect, which in quasiequilibrium is given by Fermi statistics with a suitable quasi-Fermi level. The density of electrons on defect levels follows as

$$n_d = -\frac{i}{V} \int \frac{dE}{2\pi} G_d^{<}(E), \tag{9}$$

where *V* is the volume.

In the presence of interactions such as coupling to phonons, which may change the occupation of the defect via scattering from and to the extended states, the Green's functions are modified according to the Dyson and Keldysh equations

$$G_d^{\mathrm{R,A}}(E) = \left[E \pm i\eta - \varepsilon_d - \Sigma_d^{\mathrm{R,A}}(E)\right]^{-1},\tag{10}$$

$$G_d^{\lessgtr}(E) = G_d^{\mathsf{R}}(E) \Sigma_d^{\lessgtr}(E) G_d^{\mathsf{A}}(E). \tag{11}$$

The (de)population of the defect via scattering from and to extended states in both conduction (c) and valence (v) bands may now be described by corresponding scattering

self-energies, which have the general form

$$\Sigma_{d}^{\lessgtr}(E) = \Sigma_{dc}^{\lessgtr}(E) + \Sigma_{dv}^{\lessgtr}(E)$$

$$= \sum_{\alpha, \mathbf{k}} \int d\mathbf{r} \int d\mathbf{r}' [\mathcal{M}_{dc, \pm}(\alpha, \mathbf{k}, \mathbf{r}, \mathbf{r}')]$$

$$\times G_{c}^{\lessgtr}(\mathbf{k}, \mathbf{r}, \mathbf{r}', E + E_{\alpha})$$

$$+ \mathcal{M}_{dv, \pm}(\alpha, \mathbf{k}, \mathbf{r}, \mathbf{r}') G_{v}^{\lessgtr}(\mathbf{k}, \mathbf{r}, \mathbf{r}', E - E_{\alpha})],$$
 (13)

where \mathbf{k} and \mathbf{r} , \mathbf{r}' label the periodic and nonperiodic spatial dimensions, respectively, and α denotes the degrees of freedom involved in the scattering process, e.g., phonon modes, with \mathcal{M} the associated coupling. On the other hand, the population of the extended states is also modified as a consequence of the coupling to the defect, which amounts to the renormalization of the extended state Green's functions due to the defect-related self-energies

$$\Sigma_{cd}^{\lessgtr}(\mathbf{k}, \mathbf{r}, \mathbf{r}', E) = \sum_{\alpha} \mathcal{M}_{cd, \mp}(\alpha, \mathbf{k}, \mathbf{r}, \mathbf{r}') G_d^{\lessgtr}(E - E_{\alpha}), \quad (14)$$

$$\Sigma_{vd}^{\lessgtr}(\mathbf{k}, \mathbf{r}, \mathbf{r}', E) = \sum_{\alpha} \mathcal{M}_{vd, \pm}(\alpha, \mathbf{k}, \mathbf{r}, \mathbf{r}') G_d^{\lessgtr}(E + E_{\alpha}), \quad (15)$$

which enter the steady-state equations (at fixed \mathbf{k} , E) for the extended-state Green's functions (b = c, v):

$$\int d\mathbf{r}_1 \left[\left\{ G_{b0}^R \right\}^{-1} (\mathbf{r}, \mathbf{r}_1) - \Sigma_{bd}^R (\mathbf{r}, \mathbf{r}_1) \right] G_b^R (\mathbf{r}_1, \mathbf{r}') = \delta(\mathbf{r} - \mathbf{r}'),$$
(16)

$$G_b^{\lessgtr}(\mathbf{r}, \mathbf{r}') = \int d\mathbf{r}_1 \int d\mathbf{r}_2 G_b^{\Re}(\mathbf{r}, \mathbf{r}_1) \Sigma_{bd}^{\lessgtr}(\mathbf{r}_1, \mathbf{r}_2) G_b^{\Re}(\mathbf{r}_2, \mathbf{r}').$$
(17)

The corresponding self-consistency iteration process is shown in Fig. 1, where also the scattering mediating only between band states (i.e., intraband electron-phonon and interband electron-photon) is included. This representation highlights again the compatibility of the defect-scattering scheme with the conventional self-energy treatment of scattering in band states, such as, e.g., the popular self-consistent first Born approximation (SCBA).

$$\Sigma_{dc} \longleftarrow G_c \qquad \Sigma_{cc} \qquad \text{CB states}$$

$$\left(\begin{array}{c} \Sigma_{vd} \longleftarrow G_d \longrightarrow \Sigma_{cd} & \text{defect states} \end{array} \right)$$

$$\left(\begin{array}{c} \Sigma_{vd} \longleftarrow G_d \longrightarrow \Sigma_{dv} & \text{VB states} \end{array} \right)$$

FIG. 1. Self-consistent computation of Green's functions and scattering self-energies enabling the description of nonradiative transitions via midgap defect states in a fully interacting quantum transport picture, where the band states are renormalized due to interand intraband scattering as well as coupling to contacts.

III. GENERAL STEADY STATE DEFECT RECOMBINATION RATE

For the derivation of a general expression for the rate of recombination via defects, we rewrite the band self-energies in terms of an effective emission and capture process, which results in

$$\Sigma_{cd}^{<}(\mathbf{k}, \mathbf{r}, \mathbf{r}', E) = \int d\tilde{E} \mathcal{M}_{dc}^{\mathrm{em}}(\mathbf{k}, \mathbf{r}, \mathbf{r}', \tilde{E}) G_{d}^{<}(E - \tilde{E}),$$
(18)

$$\Sigma_{cd}^{>}(\mathbf{k}, \mathbf{r}, \mathbf{r}', E) = \int d\tilde{E} \mathcal{M}_{dc}^{\text{capt}}(\mathbf{k}, \mathbf{r}, \mathbf{r}', \tilde{E}) G_d^{>}(E - \tilde{E})$$
 (19)

for the scattering of conduction band electrons due to emission from and capture into the defect state, and

$$\Sigma_{vd}^{<}(\mathbf{k}, \mathbf{r}, \mathbf{r}', E) = \int d\tilde{E} \mathcal{M}_{dv}^{\mathrm{em}}(\mathbf{k}, \mathbf{r}, \mathbf{r}', \tilde{E}) G_{d}^{<}(E + \tilde{E}),$$
(20)

$$\Sigma_{vd}^{>}(\mathbf{k}, \mathbf{r}, \mathbf{r}', E) = \int d\tilde{E} \mathcal{M}_{dv}^{\text{capt}}(\mathbf{k}, \mathbf{r}, \mathbf{r}', \tilde{E}) G_d^{>}(E + \tilde{E})$$
 (21)

for the valence band, where $\mathcal{M}_{db}^{\text{em (capt)}}$ is the square of the absolute value of the matrix element for emission (capture) of an electron from (into) the defect state into (from) an extended state in band b. Similarly, the defect self-energy for carrier capture from the conduction band into the defect becomes

$$\Sigma_{dc}^{<}(E) = \sum_{\mathbf{k}} \int d\mathbf{r} \int d\mathbf{r}' \int d\tilde{E} \mathcal{M}_{dc}^{\text{capt}}(\mathbf{k}, \mathbf{r}, \mathbf{r}', \tilde{E})$$
$$\times G_{c}^{<}(\mathbf{k}, \mathbf{r}, \mathbf{r}', E + \tilde{E}), \tag{22}$$

and the defect self-energy for carrier emission from the defect state into the conduction band is written as

$$\Sigma_{dc}^{>}(E) = \sum_{\mathbf{k}} \int d\mathbf{r} \int d\mathbf{r}' \int d\tilde{E} \mathcal{M}_{dc}^{em}(\mathbf{k}, \mathbf{r}, \mathbf{r}', \tilde{E})$$
$$\times G_{c}^{>}(\mathbf{k}, \mathbf{r}, \mathbf{r}', E + \tilde{E}). \tag{23}$$

Inserting these self-energy terms into the general expression for the electron-capture rate yields, according to the general expression for the *local* scattering rate from band into defect state in the NEGF-formalism [30],

$$R_{c\to d}(\mathbf{r}) = \sum_{\mathbf{k}} \int d\mathbf{r}' \int \frac{dE}{2\pi \, \hbar} \Sigma_{cd}^{>}(\mathbf{k}, \mathbf{r}, \mathbf{r}', E) G_c^{<}(\mathbf{k}, \mathbf{r}', \mathbf{r}, E).$$
(24)

Inserting the explicit expression for the self-energy in the equation for the *global* scattering rate

$$R_{c\to d} = \int d\mathbf{r} R_{c\to d}(\mathbf{r})$$

$$= \sum_{\mathbf{k}} \int d\mathbf{r} \int d\mathbf{r}' \int \frac{dE}{2\pi\hbar} \int d\tilde{E} \left[\mathcal{M}_{dc}^{\text{capt}}(\mathbf{k}, \mathbf{r}, \mathbf{r}', \tilde{E}) \right]$$

$$\times G_d^{>}(E - \tilde{E}) G_c^{<}(\mathbf{k}, \mathbf{r}', \mathbf{r}, E)$$

$$= \int \frac{dE'}{2\pi\hbar} G_d^{>}(E') \sum_{\mathbf{k}} \int d\mathbf{r} \int d\mathbf{r}' \int d\tilde{E} \left[\mathcal{M}_{dc}^{\text{capt}}(\mathbf{k}, \mathbf{r}, \mathbf{r}', \tilde{E}) \right]$$

$$\times G_c^{<}(\mathbf{k}, \mathbf{r}', \mathbf{r}, E' + \tilde{E})$$

$$(25)$$

$$\times G_c^{<}(\mathbf{k}, \mathbf{r}', \mathbf{r}, E' + \tilde{E})$$

$$(26)$$

$$\equiv \int \frac{dE'}{2\pi\hbar} G_d^{>}(E') \Sigma_{dc}^{<}(E') \tag{28}$$

$$=R_{d\leftarrow c} \tag{29}$$

reproduces the total capture rate for a single defect.

IV. THE "QUANTUM SRH" RECOMBINATION

Within the NEGF formalism introduced above, it is possible to derive an effective (bulk) recombination rate along the lines of the semiclassical equivalent of Shockley and Read [1]. As derived above, the expressions for the volume rates of carrier capture and emission in terms of NEGF and self-energies read

$$r_{\rm capt} \equiv R_{\rm capt}/V = \rho_d \int \frac{dE}{2\pi\hbar} G_d^{>}(E) \Sigma_{dc}^{<}(E), \qquad (30)$$

$$r_{\rm em} \equiv R_{\rm em}/V = \rho_d \int \frac{dE}{2\pi \,\hbar} G_d^{<}(E) \Sigma_{dc}^{>}(E). \tag{31}$$

where $\rho_d = N_d/V$ is the spatial density of defects. In the case of negligible contribution of (tail) states in the energy gap, the lower integration limit of the defect self-energies in (22) and (23) is set to $E_C - \varepsilon_d$, where E_C denotes the conduction band edge:

$$\Sigma_{dc}^{<}(E) = \sum_{\mathbf{k}} \int_{E_C - \varepsilon_d}^{\infty} d\tilde{E} \mathcal{M}_{dc}^{\text{capt}}(\mathbf{k}, \tilde{E}) G_c^{<}(\mathbf{k}, E + \tilde{E}), \quad (32)$$

$$\Sigma_{dc}^{>}(E) = \sum_{\mathbf{k}} \int_{E_C - \varepsilon_d}^{\infty} d\tilde{E} \mathcal{M}_{dc}^{\text{em}}(\mathbf{k}, \tilde{E}) G_c^{>}(\mathbf{k}, E + \tilde{E}). \tag{33}$$

In quasiequilibrium conditions, where the occupation of band and defect states is given by Fermi statistics with corresponding quasi-Fermi levels, e.g., $f_d = f_{\mu_d}$, we can use Eqs. (5) and (6) together with Eq. (8) and the equilibrium expressions for the conduction band state GFs

$$G_b^{<}(\mathbf{k}, E) = i f_b(E) A_b(\mathbf{k}, E), \tag{34}$$

$$G_b^{>}(\mathbf{k}, E) = -i\{1 - f_b(E)\}A_b(\mathbf{k}, E), \quad b \in \{c, v\}$$
 (35)

to write the capture volume rate as follows:

$$r_{\text{capt}} = \frac{1}{\hbar} \rho_d \left[1 - f_{\mu_d}(\varepsilon_d) \right] \sum_{\mathbf{k}} \int_{E_C}^{\infty} dE \mathcal{M}_{dc}^{\text{capt}}(\mathbf{k}, E - \varepsilon_d)$$

$$\times f_{\mu_c}(E) A_c(\mathbf{k}, E)$$
(36)

and similarly

$$r_{\text{em}} = \frac{1}{\hbar} \rho_d f_{\mu_d}(\varepsilon_d) \sum_{\mathbf{k}} \int_{E_C}^{\infty} dE \mathcal{M}_{dc}^{\text{em}}(\mathbf{k}, E - \varepsilon_d)$$
$$\times \left[1 - f_{\mu_c}(E) \right] A_c(\mathbf{k}, E). \tag{37}$$

If we neglect the dependence of the transition matrix element from crystalline momentum, $\mathcal{M}_{dc}^{\text{capt}}(\mathbf{k}, E - \varepsilon_d) \approx \tilde{\mathcal{M}}_{dc}^{\text{capt}}(E)$, the momentum integration is restricted to the spectral function and provides the density of conduction band states,

$$\mathcal{N}_c(E) = (2\pi V)^{-1} \sum_{\mathbf{k}} A_c(\mathbf{k}, E). \tag{38}$$

Thus, in this case, the net capture volume rate can be written

$$r_{\text{capt,net}} = \frac{2\pi V}{\hbar} \rho_d \int_{E_c}^{\infty} dE \, \mathcal{N}_c(E)$$

$$\times \left(\left[1 - f_{\mu_d}(\varepsilon_d) \right] f_{\mu_c}(E) \tilde{\mathcal{M}}_{dc}^{\text{capt}}(E) - f_{\mu_d}(\varepsilon_d) \left[1 - f_{\mu_c}(E) \right] \tilde{\mathcal{M}}_{dc}^{\text{em}}(E) \right). \tag{39}$$

From the requirement of detailed balance, i.e., vanishing net rate in equilibrium, where $\mu_d = \mu_c$, follows the relation between the matrix elements for capture and emission,

$$\frac{\tilde{\mathcal{M}}_{dc}^{\text{em}}(E)}{\tilde{\mathcal{M}}_{dc}^{\text{capt}}(E)} = e^{-\beta(E - \varepsilon_d)}, \quad \beta = (k_B T)^{-1}.$$
 (40)

Using the relation $1 - f_{\mu}(E) = f_{\mu}(E)e^{\beta(E-\mu)}$, the net rate of carrier capture form CB into trap states is obtained as

$$r_{\text{capt,net}} = \frac{2\pi V}{\hbar} \rho_d \left[1 - f_{\mu_d}(\varepsilon_d) \right] (1 - e^{\beta(\mu_d - \mu_c)})$$

$$\times \int_{E_c}^{\infty} dE \, \tilde{\mathcal{M}}_{dc}^{\text{capt}}(E) f_{\mu_c}(E) \mathcal{N}_c(E), \tag{41}$$

which is identical to the result obtained by Shockley and Read in Ref. [1], with the spectral capture rate $c_n(E) = \tilde{\mathcal{M}}_{dc}^{\text{capt}}(E)(2\pi V/\hbar)$. The same process applies for the capture of holes from the valence band, for which the self-energies read

$$\Sigma_{dv}^{<}(E) = \sum_{\mathbf{k}} \int_{\varepsilon_{d} - E_{V}}^{\infty} d\tilde{E} \mathcal{M}_{dv}^{\text{capt}}(\mathbf{k}, \tilde{E}) G_{v}^{<}(\mathbf{k}, E - \tilde{E}), \quad (42)$$

$$\Sigma_{dv}^{>}(E) = \sum_{\mathbf{k}} \int_{\varepsilon_d - E_V}^{\infty} d\tilde{E} \mathcal{M}_{dv}^{\text{em}}(\mathbf{k}, \tilde{E}) G_v^{>}(\mathbf{k}, E - \tilde{E}). \tag{43}$$

Here the matrix element for the emission of an electron into the valence band equals the element for the capture of a hole from the valence band, i.e., $\mathcal{M}_{dv}^{\text{em}} = \mathcal{M}_{vd}^{\text{capt}}$. The ratio of the matrix elements for electron capture and emission from and to the valence band is again fixed by the detailed balance requirement of the equilibrium situation,

$$\frac{\tilde{\mathcal{M}}_{dv}^{\text{em}}(E)}{\tilde{\mathcal{M}}_{dv}^{\text{capt}}(E)} = e^{\beta(\varepsilon_d - E)},\tag{44}$$

where the effective matrix elements are related to the coupling functions in the self-energies via the relation $\mathcal{M}_{dv}^{\text{capt}}(\mathbf{k}, \varepsilon_d - E) \approx \tilde{\mathcal{M}}_{dv}^{\text{capt}}(E)$, and to the spectral capture rate in Ref. [1] via $c_p(E) = \tilde{\mathcal{M}}_{dv}^{\text{em}}(E)(2\pi V/\hbar)$.

V. DEFECT RECOMBINATION VIA MULTIPHONON RELAXATION

An efficient process for carrier capture into localized states is the multiphonon relaxation mechanism [36]. Here we will follow the approach of Ref. [37] to implement the corresponding recombination mechanism within the NEGF picture for both spatially uniform and nonuniform situations with finite fields.

A. Coupling of flat bulk bands to an isolated defect

We will first consider the situation without spatial variation in the active device region, i.e., the scenario on which the

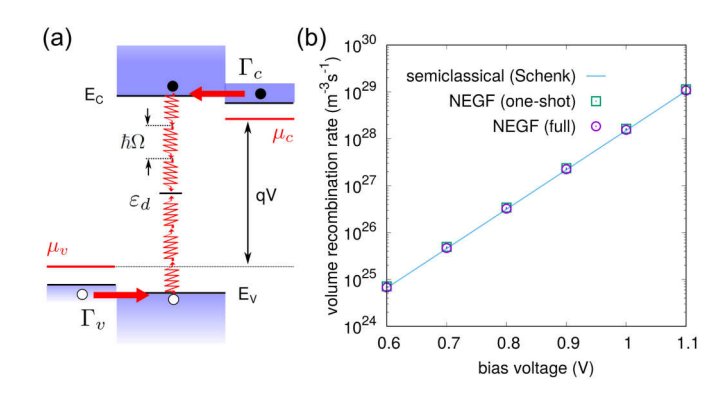


FIG. 2. (a) Schematic representation of nonradiative carrier recombination via coupling of the contacted states to defects states in the band gap through multiphonon relaxation. (b) Volume recombination rate for bulk GaAs as obtained from the semiclassical approach in Ref. [37] and from the NEGF treatment, for a single iteration of the self-consistency iteration (one shot \rightarrow Born approximation) and the full scheme. The bulk band and defect parameters used are given in Table I, and a defect concentration $\rho_d=10^{14}~{\rm cm}^{-3}$ is assumed.

original SRH model is based. The two bulk bands for electrons and holes are selectively coupled to bulk electrodes with finite bandwidth, such that no intraband current, but only interband current flow is possible, via the corresponding interband scattering process, either direct and radiative, or nonradiative via the midgap defect state. This situation is represented in Fig. 2(a).

The self-energies for multiphonon scattering entering the equations for the defect Green's function follow from Eqs. (32) and (33) and Eqs. (42) and (43) together with the matrix elements given in Appendix A,

$$\Sigma_{dc}^{<}(E) = \sum_{\mathbf{k}} \sum_{l>0} \mathcal{M}_{dc}(l) G_c^{<}(\mathbf{k}, E + l\hbar\Omega_0), \tag{45}$$

$$\Sigma_{dc}^{>}(E) = \sum_{\mathbf{k}} \sum_{l \geq 0} \mathcal{M}_{dc}(l) e^{-\beta l \hbar \Omega_0} G_c^{>}(\mathbf{k}, E + l \hbar \Omega_0) \quad (46)$$

for the coupling of the defect to the conduction band states, and

$$\Sigma_{dv}^{<}(E) = \sum_{\mathbf{k}} \sum_{l>0} \mathcal{M}_{dv}(l) e^{-\beta l \hbar \Omega_0} G_v^{<}(\mathbf{k}, E - l \hbar \Omega_0), \quad (47)$$

$$\Sigma_{dv}^{>}(E) = \sum_{\mathbf{k}} \sum_{l>0} \mathcal{M}_{dv}(l) G_{v}^{>}(\mathbf{k}, E - l\hbar\Omega_{0}) \qquad (48)$$

for the contribution of the valence band states to the defect scattering functions. The modification of the carrier Greens functions of the band states due to scattering into and from a *single* defect are encoded in the self-energies

$$\Sigma_{cd}^{<}(\mathbf{k}, E) \approx \sum_{l \geqslant 0} \mathcal{M}_{dc}(l) e^{-\beta l \hbar \Omega_0} G_d^{<}(E - l \hbar \Omega_0), \qquad (49)$$

$$\Sigma_{cd}^{>}(\mathbf{k}, E) = \sum_{l \geqslant 0} \mathcal{M}_{dc}(l) G_d^{>}(E - l\hbar\Omega_0), \tag{50}$$

TABLE I. Material parameters used in bulk simulations.

m_c^* (m_0)	m_v^* (m_0)	<i>E</i> _{c0} (eV)	<i>E</i> _{v0} (eV)	ε_d (eV)	$\sigma_{n/p}$ (cm ²)	$\hbar\Omega_0$ (meV)
0.067	0.1	1.42	0	0.71	10^{-15}	36

and

$$\Sigma_{vd}^{<}(\mathbf{k}, E) \approx \sum_{l>0} \mathcal{M}_{dv}(l) G_d^{<}(E + l\hbar\Omega_0), \tag{51}$$

$$\Sigma_{vd}^{>}(\mathbf{k}, E) = \sum_{l \geq 0} \mathcal{M}_{dv}(l) e^{-\beta l \hbar \Omega_0} G_d^{>}(E + l \hbar \Omega_0).$$
 (52)

In a first approach we assume that the defect DOS is not affected by the coupling to band states. We therefore do not solve Dyson's equation for the retarded Green's function of the defect, but use the form given in Eqs. (5) and (6) for the correlation functions based on a phenomenological spectral function $A_d(E)$, which is not renormalized. While this spectral function can have arbitrary shape, we here first consider the simplest case of a delta distribution as in Expression (8). The equation for the steady-state defect occupation function f_d is obtained by inserting the explicit expressions for the phenomenological Green's function into the expressions for net electron and hole capture and emission rates:

$$R_{dc,\text{net}}^{\text{el}} = R_{dc,\text{capt}}^{\text{el}} - R_{dc,\text{em}}^{\text{el}}$$
 (53)

$$= \int \frac{dE}{2\pi\hbar} [\Sigma_{dc}^{<}(E)G_{d}^{>}(E) - \Sigma_{dc}^{>}(E)G_{d}^{<}(E)]$$
 (54)

$$= -\frac{i}{\hbar} \left[\sum_{dc}^{<} (\varepsilon_d) \{ 1 - f_d(\varepsilon_d) \} + \sum_{dc}^{>} (\varepsilon_d) f_d(\varepsilon_d) \right]$$
 (55)

and, similarly,

$$R_{dv,\text{net}}^{\text{hl}} = R_{dv,\text{capt}}^{\text{hl}} - R_{dc,\text{em}}^{\text{hl}}$$
 (56)

$$= \int \frac{dE}{2\pi\hbar} [\Sigma_{dv}^{>}(E)G_{d}^{<}(E) - \Sigma_{dv}^{<}(E)G_{d}^{>}(E)]$$
 (57)

$$= \frac{i}{\hbar} \left[\Sigma_{dv}^{>}(\varepsilon_d) f_d(\varepsilon_d) + \Sigma_{dv}^{<}(\varepsilon_d) \{1 - f_d(\varepsilon_d)\} \right]. \tag{58}$$

The balance of these rates at the steady-state requires $R_{dc,\rm net}^{\rm el} = R_{dv,\rm net}^{\rm hl}$, which provides the following expression for the defect occupation function in terms of the scattering self-energies and the defect DOS:

$$f_d(\varepsilon_d) = -i \frac{\sum_{dc}^{\langle}(\varepsilon_d) + \sum_{dv}^{\langle}(\varepsilon_d)}{\Gamma_{dc}(\varepsilon_d) + \Gamma_{dv}(\varepsilon_d)},$$
 (59)

where $\Gamma \equiv i(\Sigma^> - \Sigma^<)$ is the lifetime broadening function associated with the respective scattering process.

Using the explicit analytical quasiequilibrium expressions (34) and (35) for the band GFs in the self-energy expressions (45)–(48), the occupation function acquires the form obtained from the standard semiclassical analysis in Ref. [1]. The numerical evaluation of the volume recombination rate is shown in Fig. 2(b) for capture cross sections obtained from the multiphonon relaxation formalism of Ref. [37] using the parameters in Table I, for monoenergetic defects at a density $\rho_d = 10^{14} \, \mathrm{cm}^{-3}$. In this case, where a flat-band bulklike density of states is considered explicitly also in the NEGF

approach, there is a close agreement of the semiclassical result (line) and the NEGF data (symbols), with only marginal impact of the additional cascade capture due to the scattering with LO-phonons in the bands (circles) over the one-shot result based on an unmodified DOS (squares).

B. Thin film devices

To include the defect-mediated recombination in realistic thin film devices, a model with spatial resolution in transport direction is required. For that purpose, the Green's functions and self-energies are written in a real-space basis reflecting the deviation from periodicity in transport direction. In this situation, the most general expression for the self-energy of carrier capture into the defect state d reads

$$\Sigma_{dc}^{<}(E) = \sum_{\mathbf{k}_{\parallel}} \int dz \int dz' \int d\tilde{E} \left[\mathcal{M}_{dc}^{\text{capt}}(\mathbf{k}_{\parallel}, z, z', \tilde{E}) \right] \times G_{c}^{<}(\mathbf{k}_{\parallel}, z, z', E + \tilde{E}) .$$
(60)

While integration over the entire longitudinal space still ensures nonlocal coupling, the off-diagonal elements of the extended-state Green's functions encoding coherence effects are not considered by using the matrix elements from Ref. [37], in which case the above self-energy acquires the following form:

$$\Sigma_{dc}^{<}(E) = \sum_{\mathbf{k}_{\parallel}} \sum_{l \geqslant 0} \mathcal{M}_{dc}(l) \int dz \, G_{c}^{<}(\mathbf{k}_{\parallel}, z, z, E + l\hbar\Omega_{0}).$$

$$\tag{61}$$

This self-energy, together with its counterpart for coupling to valence band states, is again used to compute the occupation function of a specific defect (at a specific location) according to (59). From the general form of the self-energies for extended states, we find the expressions corresponding to the quasi-1D situation, e.g.,

$$\Sigma_{cd}^{<}(\mathbf{k}_{\parallel}, z, z', E) = \int d\tilde{E} \mathcal{M}_{dc}^{em}(\mathbf{k}_{\parallel}, z, z', \tilde{E}) G_{d}^{<}(E - \tilde{E}),$$
(62)

where the spatial dependence is limited to that of the defect Green's function. In the case of local coupling to the defect at position z_0 , the self-energy can be approximated as follows:

$$\Sigma_{cd}^{<}(\mathbf{k}_{\parallel}, z, z', E) \approx \sum_{l \geqslant 0} \mathcal{M}_{dc}(l) e^{-\beta l \hbar \Omega_0} G_d^{<}(E - l \hbar \Omega_0)$$
$$\times \delta(z - z_0) \delta(z' - z_0). \tag{63}$$

In analogy to the procedure for bulk states, the *local* SRH volume rate at the defect position z_0 can be recovered if the *local* quasiequilibrium approximation is used for the Green's function in (61):

$$r_{\text{capt,net}}^{\text{el}}(z_0) \approx \rho_d(z_0)/(2\pi\hbar) \{1 - f_{\mu_d(z_0)}[\varepsilon_d(z_0)]\}$$

$$\times (1 - e^{\beta[\mu_d(z_0) - \mu_c(z_0)]}) \int_{E_C(z_0)}^{\infty} dE \, \tilde{\mathcal{M}}_{dc}^{\text{capt}}(E)$$

$$\times f_{\mu_c(z_0)}(E) \mathcal{N}_c(z_0, E), \tag{64}$$

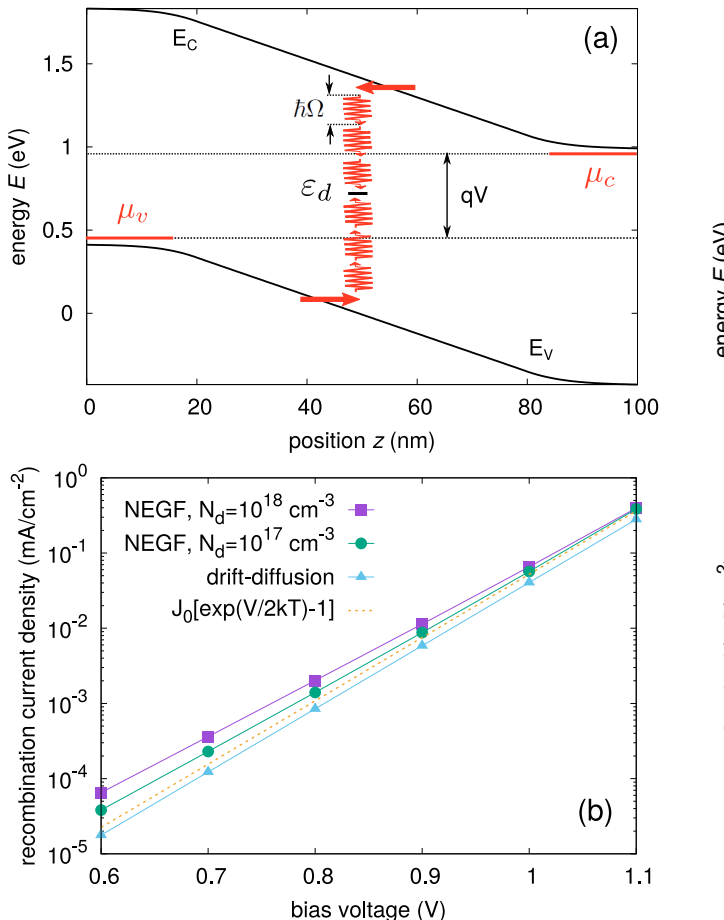


FIG. 3. (a) Band profile and schematic recombination process in a 100-nm-thick GaAs p-i-n diode with a single defect state located in the center of the intrinsic region ($z_0 = 50$ nm), displayed for a doping density of $N_{\rm dop} = 10^{18}$ cm $^{-3}$ and at 0.6 V forward bias. Electron and hole effective masses were set to $m_c^* = 0.067$ m_0 and $m_v^* = 0.22$ m_0 , respectively. (b) Recombination characteristics for $\varepsilon_d = 0.75$, $\rho_d = 10^{14}$ cm $^{-3}$, and $\sigma_n = \sigma_p = 10^{-14}$ cm $^{-2}$. For $N_{\rm dop} = 10^{18}$ cm $^{-3}$ (filled squares), the large built-in electrostatic field leads to deviations from the semiclassical characteristics (triangles) due to the enhancement of recombination by tunneling into field-induced band tails. At reduced doping of $N_{\rm dop} = 10^{17}$ cm $^{-3}$ (filled circles), the lower field moves the characteristics closer to the ideality factor of 2 (dashed line) observed in the semiclassical result.

where N is the (local) density of states given by

$$\mathcal{N}_c(z, E) = (2\pi \mathcal{A})^{-1} \sum_{\mathbf{k}_{\parallel}} A_c(\mathbf{k}_{\parallel}, z, z, E), \tag{65}$$

with A the cross section area. The spectral function itself is again related to the correlation function in the usual way for quasiequilibrium (also known as generalized Kadanoff-Baym ansatz in quantum transport [38,39])

$$G_c^{<}(\mathbf{k}_{\parallel}, z, z, E) = i f_{\mu_c(z)}(E) A_c(\mathbf{k}_{\parallel}, z, z, E). \tag{66}$$

The energetic position of the defects thereby needs to be adjusted for the local electrostatic potential affecting the band profile, i.e., $\varepsilon_d(z) = \varepsilon_{d,(0)} + U(z)$, where U is the electrostatic potential energy obtained from the solution of Poisson's equation.

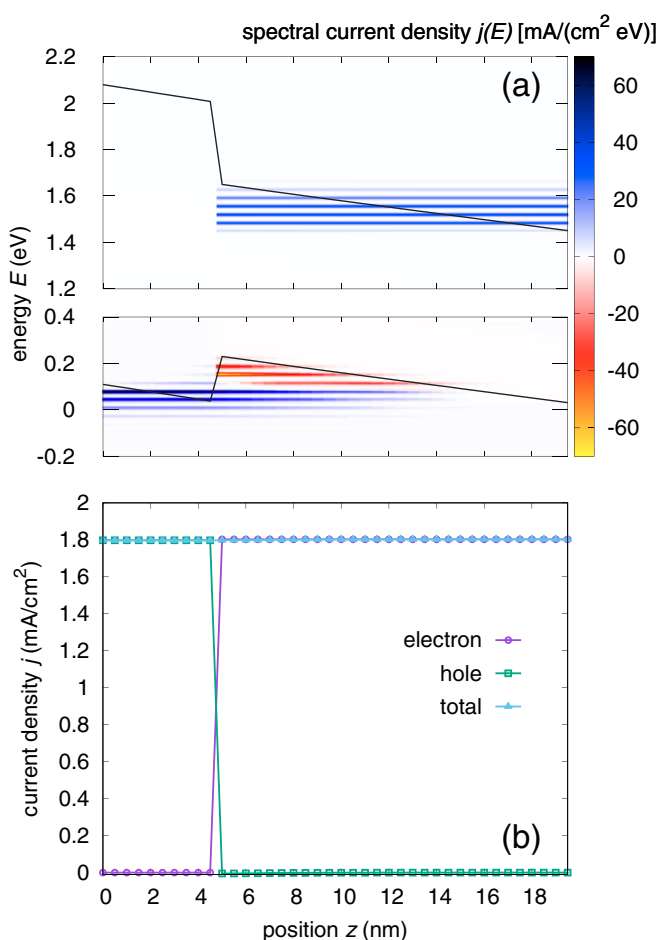


FIG. 4. (a) Spectral recombination current flow at a defective AlGaAs-GaAs heterointerface (band edge profiles indicated as gray lines). While electrons tunnel to the defect location unhindered, the holes have to overcome an injection barrier, and a reverse flow at lower energies is generated. (b) The current density as obtained from integrating the spectral current flow over energy perfectly obeys current conservation in the digital form as expected from semiclassical simulations.

As a test case we consider the recombination current generated in the dark by the presence of an ensemble of monoenergetic isolated defects in the center of the intrinisc region of an ultrathin GaAs p-i-n diode with large built-in field. The band profile of the device (for doping density of $N_{\rm dop} = 10^{18} {\rm cm}^{-3}$ and at 0.6 V forward bias) is displayed in Fig. 3(a), together with the location of the defect levels and a schematic depiction of the multiphonon recombination process. The corresponding current-voltage characteristics are displayed in Fig. 3(b) (filled squares). Comparison with the characteristics obtained from the semiclassical drift-diffusion approach (using the implementation in AFORS-HET [40]) reveals an increase of the ideality factor that originates in the tunneling of carriers into field-induced band-tail states with lower energetic separation from the defect state. Indeed, the characteristics for lower doping density of $N_{\text{dop}} = 10^{17} \text{ cm}^{-3}$ —corresponding to a lower built-in field—approach again the semiclassical ideality factor.

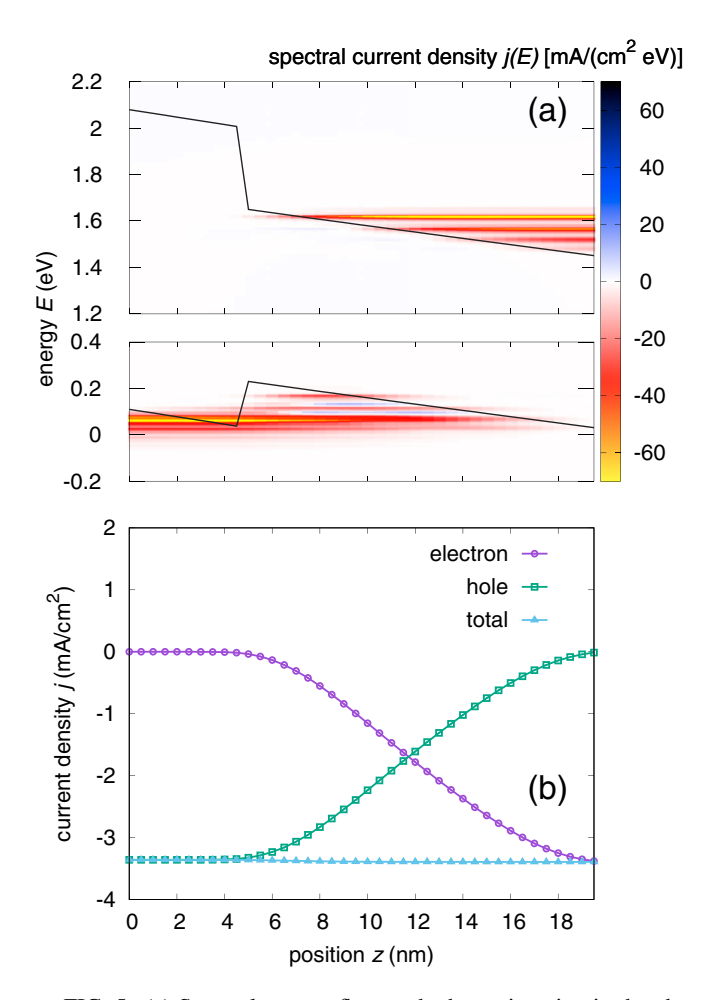


FIG. 5. (a) Spectral current flow at the heterojunction in the absence of recombination, but under illumination with monochromatic photons of energy $E_{\gamma}=1.45$ eV and at an intensity $I_{\gamma}=10$ kW/m². (b) Integrated electron, hole, and total current; the latter is again conserved over the entire structure.

Finally, and in order to apply the model in a relevant nonbulklike situation, the recombination current flow at a defective AlGaAs-GaAs heterointerface is investigated both in the dark and under illumination. The band profile of the heterointerface is shown as gray lines in Fig. 4(a). The material parameters are the same as for the *p-i-n* homojunction, with the exception of the defect density, which was increased to $\rho_d = 10^{16} \, \mathrm{cm}^{-3}$. As can be inferred from Fig. 4(a), which displays the spectral recombination current in the dark and a forward bias voltage of $V_{\rm bias} = 1.1$ V, the electron current flows unhindered and assisted by field-induced tunneling into the gap, while hole flow proceeds via hot carrier tunneling injection through the barrier, relaxation, and near-band-edge reverse flow to the heterointerface. In spite of the spectral picture of hole flow turning out to be unexpectedly complex and feature rich, the energy-integrated current density displayed in Fig. 4(b) perfectly obeys current conservation (i.e., the total current, which is the sum of electron and hole currents, is constant over the entire device) and appears in the digital form known from the semiclassical picture. In contrast to the semiclassical drift-diffusion picture that corresponds to solving a balance equation, observation of the microscopic

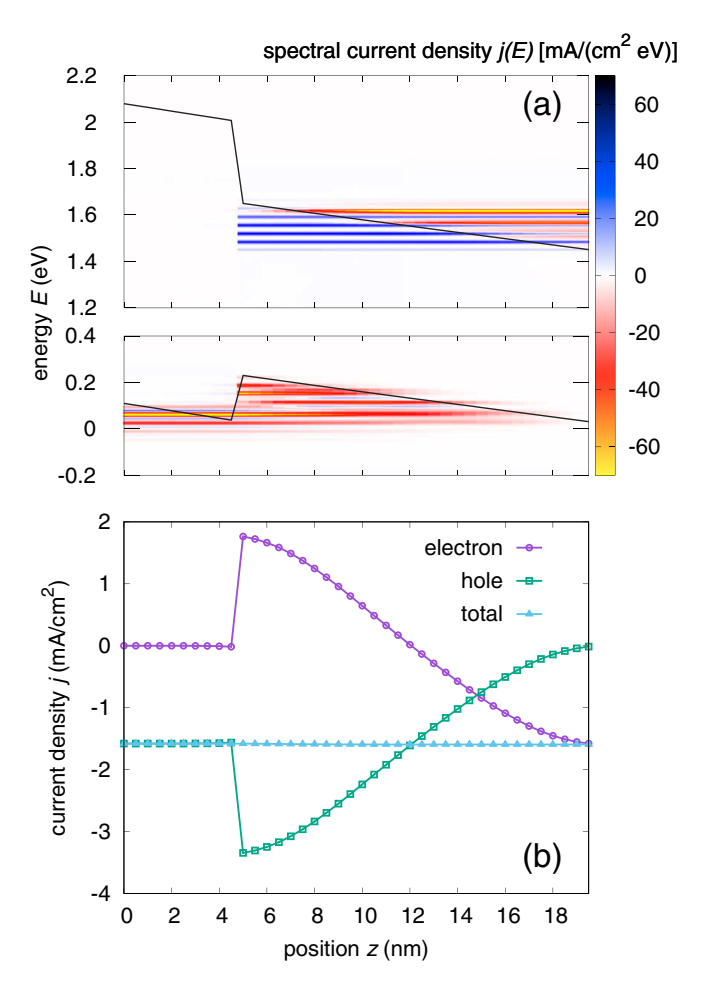


FIG. 6. Current flow at the heterointerface in the presence of both defect-mediated recombination and photocurrent generation: (a) The spectral current flow shows complex patterns due to the superposition of generation and recombination components. (b) The integrated current reflects in the electron and hole components the competing processes of carrier injection and extraction, while the total current is again perfectly conserved.

conservation law is a nontrivial feature and an excellent verification of the NEGF approach and its numerical implementation. The photocurrent generated in the same structure (without recombination) and under illumination with photons of energy $E_{\gamma} = 1.45$ eV and intensity $I_{\gamma} = 10$ kW/m² is displayed in Fig. 5. The nonlocal self-energy with coupling to the classical vector potential as derived in Ref. [31] is used to describe the electron-photon interaction. While multiphonon scattering is absent in this situation, the effects of sequential intraband electron-phonon scattering is clearly visible in the photocurrent spectra in Fig. 5(a). Again, the total integrated current is perfectly conserved. Finally, Fig. 6 displays the spectral and integral current flow at the heterointerface with both defect-mediated recombination and photocurrent generation considered. This time, the superposition of the two current components leads to a complex pattern in the spectral flow of electrons [Fig. 6(a)]. The integral current flow reflects the generation and recombination components, with the total current nonetheless observing perfect current conservation [Fig. 6(b)].

VI. CONCLUSIONS

In this paper we developed a nonequilibrium quantumstatistical description of nonradiative charge carrier recombination via localized deep defect states identified as a performance limiting process in a wide range of optoelectronic devices. Based on a conserving scattering self-energy defined within the NEGF framework, it is fully compatible with NEGF simulations of charge carrier photogeneration, radiative recombination, and transport, and thus represents an essential element of a comprehensive NEGF picture of quantum-optoelectronic device operation. Numerical simulations based on the formalism reveal nonclassical behavior even for simple structures, such as recombination enhancement due to tunneling into field-induced band-tail states, or tunneling injection and complex reverse carrier flow close to defective heterointerfaces. This enables the rigorous assessment of nonradiatively limited device architectures that are not accessible to semiclassical simulation approaches. In the photovoltaic application field for instance, it permits the investigation of selectivity, i.e., the competition between carrier recombination and extraction, in contact configurations where transport relies largely on tunneling, as in the tunnel oxide passivated contact scheme (TOPCon) relevant for the implementation of high-efficiency silicon solar cells [41].

ACKNOWLEDGMENTS

This work was supported by the Energy oriented Centre of Excellence (EoCoE), Grant Agreement No. 676629, funded within the Horizon 2020 framework of the European Union, and benefited from COST action MP1406 – MultiscaleSolar as well as from compute time granted on the supercomputer JURECA at the Jülich Supercomputing Centre (JSC).

APPENDIX A: MULTIPHONON MATRIX ELEMENT

The matrix elements for multiphonon relaxation (MPR) are defined as in Ref. [37]. There the local element for electron capture into a defect state localized at $z = z_d$ is derived as the global quantity [42]

$$\mathcal{M}_{dc}^{\text{capt}}(\mathbf{k}, E) \approx \hbar c_n [E + \varepsilon_d(z_d)]$$
 (A1)

$$= \hbar c_{n0} \left(r_{F,n}^2 + \frac{(S\hbar\Omega_0 - E)^2}{S(\hbar\Omega_0)^2} r_{ph,n}^2 \right) L(E), \quad (A2)$$

with

$$L(E) = 2\pi \hbar e^{-S(2f_B+1)} \sum_{l=-\infty}^{\infty} \left(\frac{f_B+1}{f_B}\right)^{l/2}$$
$$\times I_l[2S\sqrt{f_B(f_B+1)}]\delta(l\hbar\Omega_0 - E), \tag{A3}$$

where S is the Huang-Rhys factor [43], I_l is the modified Bessel function, $r_{\mathrm{F},n}$ and $r_{\mathrm{ph},n}$ are matrix elements of the nondiagonal electron-field and electron-phonon coupling, respectively, and Ω is the frequency of the vibrational mode with occupation f_B . The prefactor c_{n0} contains various unknown quantities, such as the impurity potential strength, the symmetry of the wave function, etc., and will thus be used as an adjustable parameter to reproduce experimentally observed recombination rates.

The resulting effective matrix elements to be inserted in the expressions for the self-energies are then approximated as

$$\mathcal{M}_{dc}^{\text{capt}}(\mathbf{k}, E) \approx \sum_{l \ge 0} \mathcal{M}_{dc}(l) \delta(l\hbar\Omega_0 - E),$$
 (A4)

with

$$\mathcal{M}_{dc}(l) \approx \mathcal{M}_{dc}^0 \left(r_{\mathrm{F},n}^2 + \frac{(l-S)^2}{S} r_{\mathrm{ph},n}^2 \right) L(l),$$
 (A5)

where $\mathcal{M}_{dc}^0 = 2\pi \hbar^2 c_n^0$ and

$$L(l) = e^{-S(2f_B+1)} \left(\frac{f_B+1}{f_B}\right)^{l/2} I_l[2S\sqrt{f_B(f_B+1)}].$$
 (A6)

The matrix element for thermal emission of an electron from the defect into the conduction band is obtained from the capture element via the equilibrium relation (40), which yields

$$\mathcal{M}_{dc}^{\text{em}}(\mathbf{k}, E) = \mathcal{M}_{dc}^{\text{capt}}(\mathbf{k}, E)e^{-\beta E}.$$
 (A7)

Similarly, the hole capture matrix element is expressed as

$$\mathcal{M}_{dv}^{\text{em}}(\mathbf{k}, E) \approx \hbar c_p [\varepsilon_d(z_d) - E]$$
 (A8)

$$= \sum_{l \geqslant 0} \mathcal{M}_{dv}(l)\delta(l\hbar\Omega_0 + E), \qquad (A9)$$

with

$$\mathcal{M}_{dv}(l) \approx \mathcal{M}_{dv}^0 \left(r_{\mathrm{F},p}^2 + \frac{(l+S)^2}{S} r_{\mathrm{ph},p}^2\right) L(l),$$
 (A10)

where $\mathcal{M}_{dv}^0=2\pi\hbar^2c_p^0$. The matrix element for hole emission from the trap to the valence band follows again via $\mathcal{M}_{dv}^{\mathrm{capt}}(\mathbf{k},E)=\mathcal{M}_{dv}^{\mathrm{em}}(\mathbf{k},E)e^{-\beta E}$.

APPENDIX B: PARAMETRIZATION

Here the extraction of the unknown material constants in the MPR matrix element is performed via the fitting to experimentally determined capture cross sections from the literature. In the original paper by Shockley and Read [1], the recombination rate is parametrized in terms of carrier-specific rate coefficients $C_s = N_t \langle c_s \rangle$ (s = n, p), where the average capture coefficients (with units of m³ s⁻¹) are given by the following expressions:

$$\langle c_n \rangle = \int_{E_c}^{\infty} dE \{ e^{(E_c - E)/(k_B T)} c_n(E) \mathcal{N}_c(E) \} / \mathcal{N}_{c,\text{eff}}, \quad (B1)$$

$$\langle c_p \rangle = \int_{-\infty}^{E_v} dE \{ e^{(E - E_v)/(k_B T)} c_p(E) \mathcal{N}_v(E) \} / \mathcal{N}_{v,\text{eff}}.$$
 (B2)

The microscopic expressions for the energy-dependent capture coefficients $c_{n,p}(E)$ can be inferred from Eqs. (A1) and (A8), respectively. If the assumption of small ratio $r_{\rm F}/r_{\rm ph}$ from Ref. [37] is used, the unknown material parameters of the interaction with the defect can be absorbed into a single parameter $\tilde{\mathcal{M}}^0_{dc/dv} = \mathcal{M}_{dc/dv} r^2_{{\rm ph},n/p}$. This is then fixed by experimental values of capture cross sections $\sigma_{n/p}$ via the relation $\langle c_{n/p} \rangle = v_{\rm th,n/p} \sigma_{n/p}$, where $v_{\rm th}$ is the thermal velocity.

- [1] W. Shockley and W. T. Read, Phys. Rev. 87, 835 (1952).
- [2] R. Hall, Phys. Rev. 87, 387 (1952).
- [3] L. Shi and L.-W. Wang, Phys. Rev. Lett. **109**, 245501 (2012).
- [4] A. Alkauskas, Q. Yan, and C. G. Van de Walle, Phys. Rev. B 90, 075202 (2014).
- [5] C. Buurma, S. Krishnamurthy, and S. Sivananthan, J. Appl. Phys. 116, 013102 (2014).
- [6] L. Shi, K. Xu, and L.-W. Wang, Phys. Rev. B 91, 205315 (2015).
- [7] G. D. Barmparis, Y. S. Puzyrev, X.-G. Zhang, and S. T. Pantelides, Phys. Rev. B 92, 214111 (2015).
- [8] A. Alkauskas, C. E. Dreyer, J. L. Lyons, and C. G. Van de Walle, Phys. Rev. B 93, 201304 (2016).
- [9] J.-H. Yang, L. Shi, L.-W. Wang, and S.-H. Wei, Sci. Rep. 6, 21712 (2016).
- [10] J. Bang, Y. Y. Sun, J.-H. Song, and S. B. Zhang, Sci. Rep. 6, 24404 (2016).
- [11] W. Li, Y.-Y. Sun, L. Li, Z. Zhou, J. Tang, and O. V. Prezhdo, J. Am. Chem. Soc. 140, 15753 (2018).
- [12] M. F. Pereira and K. Henneberger, Phys. Rev. B 58, 2064 (1998).
- [13] L. E. Henrickson, J. Appl. Phys 91, 6273 (2002).
- [14] S.-C. Lee and A. Wacker, Phys. Rev. B 66, 245314 (2002).
- [15] D. A. Stewart and F. Leonard, Nano Lett. 5, 219 (2005).
- [16] M. A. Naser, M. J. Deen, and D. A. Thompson, J. Appl. Phys. 102, 083108 (2007).
- [17] U. Aeberhard and R. H. Morf, Phys. Rev. B 77, 125343 (2008).
- [18] S. Steiger, R. G. Veprek, and B. Witzigmann, in *Proceedings 2009 13th International Workshop on Computational Electronics*, *IWCE 2009* (IEEE, Piscataway, NJ, 2009).
- [19] T. Kubis, C. Yeh, P. Vogl, A. Benz, G. Fasching, and C. Deutsch, Phys. Rev. B 79, 195323 (2009).
- [20] U. Aeberhard, Nanoscale Res. Lett. 6, 242 (2011).
- [21] U. Aeberhard, Opt. Quantum. Electron. 44, 133 (2012).
- [22] A. Buin, A. Verma, and S. Saini, J. Appl. Phys. 114, 033111 (2013).

- [23] N. Cavassilas, C. Gelly, F. Michelini, and M. Bescond, IEEE J. Photovolt. 5, 1621 (2015).
- [24] A. Berbezier and U. Aeberhard, Phys. Rev. Appl. 4, 044008 (2015).
- [25] U. Aeberhard, IEEE J. Photovolt. 6, 654 (2016).
- [26] U. Aeberhard, A. Gonzalo, and J. M. Ulloa, Appl. Phys. Lett. 112, 213904 (2018).
- [27] U. Aeberhard, J. Comput. Electron. 10, 394 (2011).
- [28] U. Aeberhard, J. Phys. D: Appl. Phys. 51, 323002 (2018).
- [29] U. Aeberhard, MRS Proc. 1493, 91 (2013).
- [30] U. Aeberhard, Phys. Rev. B 84, 035454 (2011).
- [31] U. Aeberhard, Phys. Rev. B 89, 115303 (2014).
- [32] S. Datta, *Electronic Transport in Mesoscopic Systems* (Cambridge University Press, Cambridge, 1995).
- [33] S. Datta, *Quantum Transport* (Cambridge University Press, Cambridge, 2005).
- [34] U. Aeberhard, Appl. Phys. Lett. 109, 033906 (2016).
- [35] Spin is not treated explicitly here, as in the original approach by Shockley and Read [1].
- [36] P. T. Landsberg, Recombination in Semiconductors (Cambridge University Press, Cambridge, 1991).
- [37] A. Schenk, J. Appl. Phys. 71, 3339 (1992).
- [38] L. P. Kadanoff and G. Baym, Quantum Statistical Mechanics (Benjamin, Reading, MA, 1962).
- [39] P. Lipavský, V. Špička, and B. Velický, Phys. Rev. B 34, 6933 (1986).
- [40] A. Froitzheim, R. Stangl, M. Kriegel, L. Elstner, and W. Fuhs, in *Proceedings of the WCPEC-3, 3rd World Conference on Photovoltaic Energy Conversion, Osaka, Japan* (WCPEC-3 Organizing Committee, 2003).
- [41] F. Feldmann, G. Nogay, P. Löper, D. L. Young, B. G. Lee, P. Stradins, M. Hermle, and S. W. Glunz, Solar Energy Mater. Solar Cells 178, 15 (2018).
- [42] The deviations from the expression in Ref. [37] stem from the position of the energy zero at the defect energy.
- [43] K. Huang and A. Rhys, Proc. R. Soc. London Sect. A 204, 406 (1950).